

Shil'nikov's Theorem—A Tutorial

Christopher P. Silva, *Member, IEEE*

Abstract— The phenomenon of chaos has been observed in many nonlinear deterministic systems in both experimental and computer-simulation contexts. Given the nature of this phenomenon, however, an analytical tool is needed to ensure that what is observed is not an artifact of the device used to measure or simulate the given system. This paper provides a tutorial look at one of the few and most useful of such tools: Shil'nikov's theorem and its various extensions. This exposition presents the basic terminology and concepts related to Shil'nikov's results, a formal statement and subsequent discussion of its two basic versions for 3-D systems, as well as two example applications of Shil'nikov's method to a piecewise-linear system.

I. INTRODUCTION

THE APPARENTLY random phenomenon of chaos has become increasingly observed in the behavior of myriad *nonlinear* deterministic systems, that is, those described accurately by partial or ordinary differential equations or difference equations. These observations are being made not only experimentally, but also in computer simulations. Examples abound in a wide gamut of disciplines ranging from solid-state physics to cosmology, from electrical engineering to biology. Chaos is found in systems that are forced or unforced (also known as *nonautonomous* or *autonomous*, respectively), lossless or dissipative, discrete in time and of any dimension, or continuous in time and of dimension three or higher. A 2-D glimpse of this phenomenon is shown in Fig. 1, which depicts a simulation of the nonlinear, third-order, autonomous, dissipative electrical circuit known as Chua's circuit (which will be discussed in Example 2.1).

As the study of chaos evolved, a working definition was developed that is used to this day. A dynamical system is informally called chaotic if it contains bounded behavior exhibiting several fundamental features, three of which are as follows:

- 1) *A basically continuous, and possibly banded, Fourier or power spectrum.* This property indicates that the motion is nonperiodic and justifies the often-made analogy of chaos with noise.
- 2) *Nearby orbits that diverge exponentially fast, thus causing an extreme sensitivity to initial conditions.* Although this attribute is shared by many dynamical systems and does contribute to highly complicated dynamics, it alone does not guarantee chaotic behavior.
- 3) *Ergodicity and mixing of the orbits in the bounded portion B of the phase space where the orbits exist.* The first characteristic implies that any given orbit explores all

Manuscript received April 5, 1993; revised May 24, 1993. This paper was recommended by Guest Editor L. O. Chua.

The author is with the Electronics and Sensors Division, The Aerospace Corporation, Los Angeles, CA 90009-2957.
IEEE Log Number 9211605.

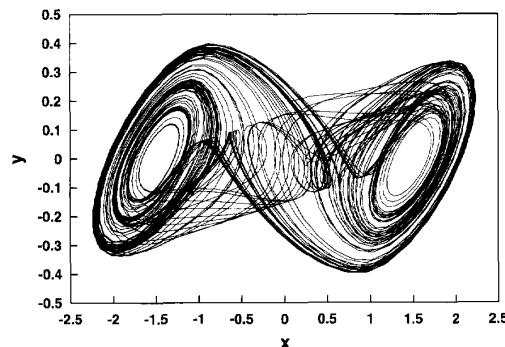


Fig. 1. Computer-simulated view of the complex bounded behavior that is the hallmark of chaos. The view is constructed by plotting two of the three state variables against each other (in this case the normalized form of the capacitor voltages in Chua's circuit) with time as the parameter. This "set of chaotic orbits" is termed a *strange attractor* because outside trajectories are typically drawn into its vicinity in the steady state.

of B . The second means that the simple relationships between initial points in any finite portion of B are essentially eliminated by the dispersive dynamics.

The above working definition of chaos has recently been formalized by Wiggins [1] for both discrete and continuous systems. Upon closer inspection of the above properties, however, an important objection might be raised: Because computer simulations have finite precision and experimental measurements have finite ranges (e.g., time or frequency), might not the behavior witnessed be either an artifact of the observation device, or might it not be actually regular but with a period or bandwidth beyond the limits capturable by the device? In fact, cases have arisen in which supposed chaotic behavior turned out to be a periodic orbit with a very long period. To allay these anxieties, an analytical approach is needed that guarantees that chaotic behavior exists in a formal sense. One of the most useful exponents of such a tool for autonomous systems is based on the fundamental work of Shil'nikov [2], [3] and subsequent embellishments and extensions. We will collectively term these approaches the *Shil'nikov method*.

In order to keep this presentation brief, we will restrict our scope to 3-D dissipative continuous systems. However, there are also Shil'nikov results for higher dimensional systems and those that are lossless (see Wiggins [4] for a detailed overview of such findings). We will begin with a self-contained description of the basic concepts and terminology needed to understand the results of Shil'nikov theory. A formal statement of two basic varieties of the Shil'nikov method, as well as two example applications, will be presented. The tutorial will close with a discussion of topics for further pursuit.

II. THE SHIL'NIKOV METHOD

A. Basic Concepts and Terminology

Consider the third-order dynamical system

$$\frac{d\mathbf{x}}{dt} = \xi(\mathbf{x}), \quad t \in \mathbf{R}, \quad \mathbf{x} \in \mathbf{R}^3 \quad (1)$$

where the vector field $\xi: \mathbf{R}^3 \rightarrow \mathbf{R}^3$ is p -times differentiable ($p \geq 1$) with a continuous derivative (called *class C^p*), and \mathbf{R}^3 stands for the real space of dimension three. Denote by $\phi^t(x)$ the *flow* of (1), that is, given the initial condition $\mathbf{x}(0) = \mathbf{x}_0$, $\phi^t(\mathbf{x}_0)$ denotes the position of the orbit originating from \mathbf{x}_0 at time t . We say that $\mathbf{x}_e \in \mathbf{R}^3$ is an *equilibrium point* for (1) if $\xi(\mathbf{x}_e) = \mathbf{0}$ because the \mathbf{x} -motion is seen to be fixed at \mathbf{x}_e for all time. We call an equilibrium point \mathbf{x}_e for (1) a *hyperbolic saddle focus* (or *saddle focus*, for short) if the eigenvalues of the 3×3 real matrix $D\xi(\mathbf{x}_e)$, the Jacobian derivative of ξ at \mathbf{x}_e , are of the form

$$\gamma, \sigma \pm j\omega, \sigma\gamma < 0, \omega \neq 0 \quad (2)$$

where γ, σ , and ω are real. Associated with this equilibrium point will be a 2-D *eigenplane* $E^c(\mathbf{x}_e)$ corresponding to the complex conjugate eigenvalues $\sigma \pm j\omega$ and a 1-D *eigenline* $E^r(\mathbf{x}_e)$ corresponding to the real eigenvalue γ . These sets will be *invariant* to the flow of the *linearized dynamical system*

$$\frac{d\mathbf{x}}{dt} = D\xi(\mathbf{x}_e)\mathbf{x} \quad (3)$$

which approximates (1) near \mathbf{x}_e . This means that an orbit of (3) that initiates in these sets will remain in them for all forward or reverse time thereafter. The motion in $E^c(\mathbf{x}_e)$ will be that of the usual stable or unstable focus, depending on whether σ is negative or positive, respectively, while the motion in $E^r(\mathbf{x}_e)$ will obviously be along a line with a direction that is determined by the sign of γ .

Fig. 2 presents the two very special orbits that lie at the heart of the Shil'nikov approach. By a *homoclinic orbit* we mean a bounded dynamical trajectory of (1) that is *doubly asymptotic* to an equilibrium point (that is, as time approaches $\pm\infty$; see Fig. 2(a) for the case of a saddle focus). A *heteroclinic orbit* is similar except that there are two distinct saddle foci being connected, one corresponding to the forward asymptotic time limit and the other to the reverse asymptotic time limit (see Fig. 2(b)). A *heteroclinic loop* is formed by the union of two or more heteroclinic orbits (see Fig. 2(b)). We will use the term *Shil'nikov system* when referring to (1), where these special orbits based at saddle-focus-type equilibrium points are present in the dynamics.

Another important concept needed here is that of a *Poincaré map*, which is a stroboscopic means of analyzing the dynamics of certain nonlinear systems. For (1), this technique amounts to using a plane $\Sigma \subset \mathbf{R}^3$ to cut transversely across recurrent behavior (as occurs local to a homoclinic or heteroclinic orbit); this in turn defines a 2-D map $P: U \subset \Sigma \rightarrow \Sigma$, called the Poincaré map, where the neighborhood U designates those points that return to Σ at least once under the flow. This map takes a point \mathbf{x}_0 in U to the first intersection $P(\mathbf{x}_0) = \phi^{t_r}(\mathbf{x}_0)$ of the dynamical orbit from \mathbf{x}_0 with the Σ -plane (t_r is the

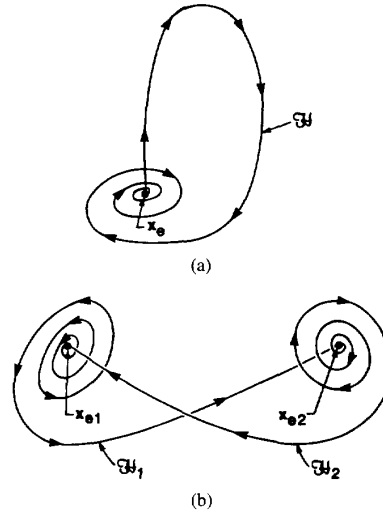


Fig. 2. Illustration of typical homoclinic and heteroclinic orbits in \mathbf{R}^3 . The arrowheads indicate the forward evolution of time. (a) Homoclinic orbit \mathcal{H} based at a hyperbolic saddle focus \mathbf{x}_e having a positive real equilibrium eigenvalue (the other case is similar). The existence of this orbit forms the basis of the homoclinic Shil'nikov method (Theorem 2.1). (b) Heteroclinic loop \mathcal{H}_1 that includes the two heteroclinic orbits \mathcal{H}_1 and \mathcal{H}_2 and the two distinct hyperbolic saddle foci \mathbf{x}_{e1} and \mathbf{x}_{e2} having negative real equilibrium eigenvalues (the other case is similar). The existence of this loop forms the basis for the heteroclinic Shil'nikov method (Theorem 2.2).

transit time for this orbit).¹ Fig. 3 depicts a case in which a Poincaré map is constructed in the neighborhood of a periodic orbit Δ (which itself is seen to correspond to a *first-order fixed point* of P , that is, $P(\mathbf{x}_*) = \mathbf{x}_*$). Observe that P defines a 2-D discrete dynamical system

$$\mathbf{x}_{k+1} = P(\mathbf{x}_k), \quad k = 0, 1, \dots \quad (4)$$

that characterizes (1). With this approach, one may then study the reduced system in (4) instead of the original 3-D system in (1). For example, the stability properties of Δ are reflected in the stability of the fixed point \mathbf{x}_* . For the case of a homoclinic orbit (a heteroclinic orbit or loop is similar), a characteristic local Poincaré map P (called the *Shil'nikov map*) can be constructed from two constituent maps: ψ_e , which corresponds to the linearized flow near the equilibrium point (that is, the flow governed by (3)), while the second one, ψ_h , describes the behavior in a neighborhood of the homoclinic orbit away from the equilibrium point (see Fig. 4).

The final concept needed here is that of the *Smale horseshoe map* and its associated invariant 2-D set Λ , called the *Smale horseshoe* (see [5]). This is the set analytically detected by the Shil'nikov method in the discrete dynamics generated by the Shil'nikov map (that is, in (4)), and which guarantees that the original system [equation (1)] is chaotic in a rigorous sense. In fact, it can be shown that when the Smale horseshoe Λ is

¹Note that if $P(\mathbf{x}_0) \notin U$, then $P^{(2)}(\mathbf{x}_0) = P \circ P(\mathbf{x}_0)$ will not be defined. This "escape" of \mathbf{x}_0 from U can occur for any higher number of iterations under P .

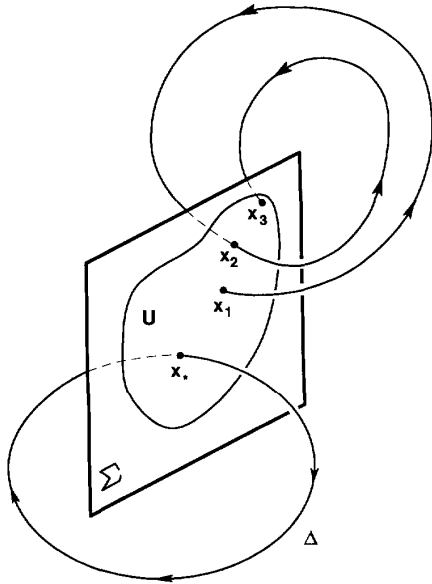


Fig. 3. Illustration of the Poincaré map $P: U \rightarrow \Sigma$ local to a periodic orbit Δ . We call the plane Σ a *local cross section* at x_* . The transversality of Σ to the flow means that $\xi(x)$ is not parallel to Σ for all x in Σ . A sample orbit initiating at $x_1 \in \Sigma$ and intersecting Σ twice more at x_2 and x_3 is shown. In terms of P , this implies that $x_2 = P(x_1)$, $x_3 = P(x_2)$, and hence, $x_3 = P^{(2)}(x_1)$.

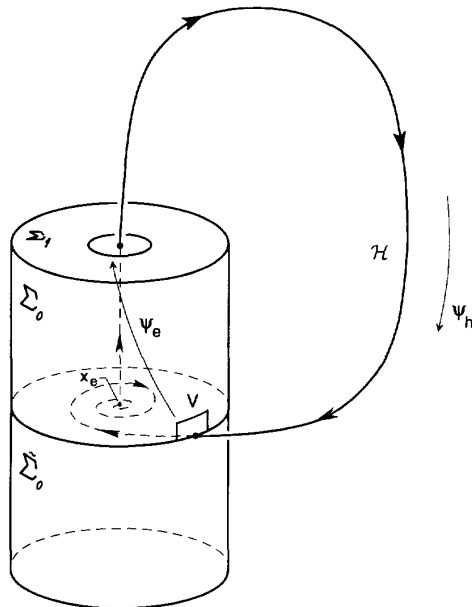


Fig. 4. The Shil'nikov map $P: V \rightarrow \Sigma_0 \cup \tilde{\Sigma}_0$ for the case of a homoclinic orbit \mathcal{H} based at the saddle focus x_e . Here, V is a small section of the cylindrical surface Σ_0 . The map $\psi_e: \Sigma_0 \rightarrow \Sigma_1$ characterizes the behavior local to x_e , whereas $\psi_h: \Sigma_1 \rightarrow \Sigma_0 \cup \tilde{\Sigma}_0$ takes care of the behavior local to the portion of \mathcal{H} that is not in the neighborhood of x_e .

embedded in (4), then there exist the following orbits in (1) that typify chaotic behavior:

- 1) a *countable* infinity (that is, the number can be put in one-to-one correspondence with the natural numbers) of periodic orbits consisting of orbits of all periods
- 2) an *uncountable* infinity (that is, the number can be put in one-to-one correspondence with the real numbers) of nonperiodic orbits
- 3) a *dense* orbit, that is, one that passes arbitrarily closely to any point in Λ .

In its simplest form, the Smale horseshoe map can be written as $f_s: S \rightarrow \mathbf{R}^2$, where S is the unit square in \mathbf{R}^2 . Its basic operation (see Fig. 5) is that of contracting S in the x -direction, expanding it in the y -direction, folding the result (which is in the shape of a horseshoe), and placing this result back over S . Note how pieces of S fall outside of S under the action of f_s , and how the horizontal rectangles H_0 and H_1 become the vertical ones V_0 and V_1 , respectively. By repeating iterations under f_s , which corresponds to evolving the discrete dynamics generated by f_s , and retaining only those points in S that remain invariant under f_s , one arrives at a very complex set of points in S (in the limit of an infinite number of iterations) that is the Smale horseshoe. This set is reminiscent of a 2-D version of the familiar *Cantor set* (wherein the middle-third interval is removed from the unit interval, the same is done for the remaining two subintervals, and this process is repeated *ad infinitum*). The basic process of the Shil'nikov method is then to show that the Shil'nikov map behaves qualitatively the same as the map f_s , thereby ensuring the existence of the Smale horseshoe in the map's discrete dynamics—and hence finally *horseshoe chaos* in the original third-order continuous system, as indicated above.

B. Formal Statement of Results

Given the background just presented, we are now ready to state the two basic versions of the Shil'nikov method: one based on the presence of a homoclinic orbit and one assuming the existence of a heteroclinic loop.

Theorem 2.1 (Homoclinic Shil'nikov Method): Given the third-order autonomous system in (1), where ξ is a C^2 vector field on \mathbf{R}^3 . Let x_e be an equilibrium point for (1). Suppose the following:

- 1) The equilibrium point is a saddle focus whose characteristic eigenvalues satisfy the *Shil'nikov inequality*, that is,

$$|\gamma| > |\sigma| > 0. \tag{5}$$

- 2) There exists a homoclinic orbit \mathcal{H} based at x_e .

Then

- 1) The Shil'nikov map defined in a neighborhood of \mathcal{H} possesses a countable number of Smale horseshoes in its discrete dynamics.
- 2) For any sufficiently small C^1 -perturbation ζ of ξ^2 , the perturbed system

$$\frac{dx}{dt} = \zeta(x), \quad x \in \mathbf{R}^3 \tag{6}$$

²Roughly, this means that the norm of the difference $\xi - \zeta$ and its first derivative are sufficiently small in a neighborhood containing \mathcal{H} .

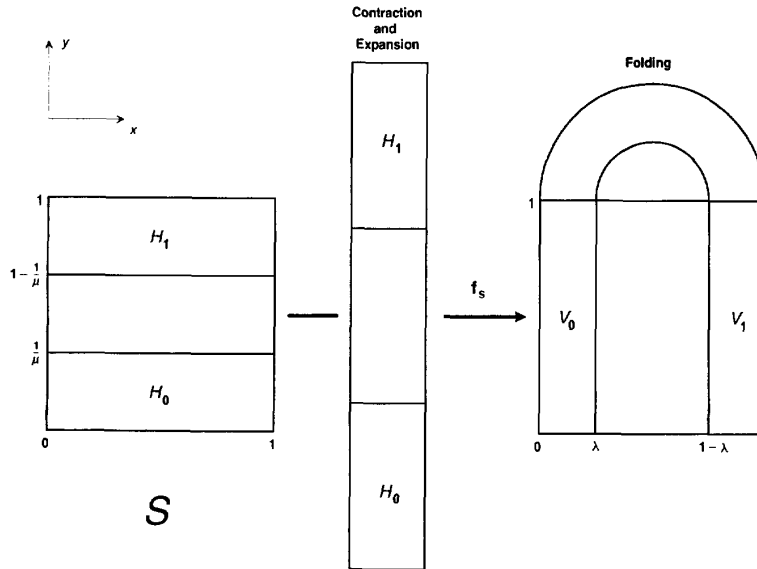


Fig. 5. Geometric illustration of the simplified Smale horseshoe map f_s . Its basic characteristics of 1) mapping disjoint regions (such as H_0 and H_1) over themselves (note $V_i := f_s(H_i)$, $i = 0, 1$) and 2) "strong" stretching and contraction in complementary directions are representative of the Poincaré maps for many of the continuous dynamical systems that exhibit chaotic behavior.

has at least a finite number of Smale horseshoes in the discrete dynamics of the Shil'nikov map defined near \mathcal{H} .

- 3) Both the original system [equation (1)] and the perturbed one [equation (6)] exhibit horseshoe chaos (also known as *homoclinic chaos*).

Remarks

- i) This result was put forth originally by Shil'nikov, with the Smale horseshoe aspects added later. It has also been extended to piecewise- C^2 vector fields (that is, vector fields that are C^2 in pieces that are regions whose union is \mathbb{R}^3), provided that 1) \mathbf{x}_e is in the interior of one of the pieces, and 2) \mathcal{H} is bounded away from any equilibrium point other than \mathbf{x}_e and is not tangent to any of the boundary surfaces between the pieces. The details of this extension can be found in [6].
- ii) Conclusions 2 and 3 indicate what is called the *structural stability property* of homoclinic chaos, that is, it remains in existence despite minor changes in the vector field. This has important implications for both the numerical and experimental investigation of chaos, since the environmental parameters in these contexts do vary with time and are known to only a finite precision. Unlike homoclinic chaos, the existence of the homoclinic orbit itself is *not* guaranteed to be structurally stable.
- iii) It turns out that the (first) Shil'nikov inequality in (5) is very crucial, in that if it is reversed, the Smale horseshoes go away and no chaos appears. The boundary $|\sigma| = |\gamma|$ is an interesting *bifurcation point* between regular and chaotic behavior.
- iv) The most difficult part of applying this method is the formal establishment of the homoclinic orbit's exis-

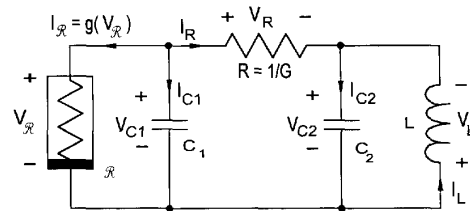


Fig. 6. Chua's circuit, an example system for which the Shil'nikov method can be applied. The only nonlinear element is the resistor \mathcal{R} , which has a piecewise-linear current/voltage characteristic and is locally active.

tence. The following example indicates how this can be done for the case of a piecewise-linear system.

Example 2.1 (Chua's Circuit: Homoclinic Orbit from a Saddle Focus): Chua's circuit, shown in Fig. 6, has become a paradigm for chaos, being one of the simplest systems manifesting the complex phenomenon of chaos in both laboratory and computer environments (see [7]). The only nonlinear element in this third-order circuit is the active piecewise-linear resistor \mathcal{R} , which is described through the relation

$$g(v_{\mathcal{R}}) = \begin{cases} m_1 v_{\mathcal{R}} + B_p(m_0 - m_1), & v_{\mathcal{R}} \geq B_p \\ m_0 v_{\mathcal{R}}, & |v_{\mathcal{R}}| \leq B_p \\ m_1 v_{\mathcal{R}} - B_p(m_0 - m_1), & v_{\mathcal{R}} \leq -B_p \end{cases} \quad (7)$$

where m_0 and m_1 are negative slopes and B_p is a breakpoint parameter. For the practical realization of the circuit, this resistor must be eventually passive for $|v_{\mathcal{R}}|$ on the order of several volts. In this way, the experimental observation of chaos will match the computer one made using the ideal globally active characteristic in (7).

A formal analysis of the general double-scroll vector field family (which contains Chua's circuit as a special case) is

given in [8], which includes a general qualitative analysis culminating in a demonstration of the presence of homoclinic chaos, along with a detailed bifurcation analysis (wherein the qualitative behavior is studied as a circuit parameter is varied). The vector fields here are 1) piecewise-linear (and hence piecewise C^∞ (smooth)), consisting of three regions with two parallel planes as the boundary surfaces, and 2) are odd symmetric with respect to the origin. This can be readily seen from the dimensionless form of the state equation, which is given by

$$\begin{aligned}\frac{dx}{d\tau} &= \alpha[y - x - f(x)] \\ \frac{dy}{d\tau} &= x - y + z \\ \frac{dz}{d\tau} &= -\beta y\end{aligned}\quad (8a)$$

where

$$f(x) = \begin{cases} bx + a - b, & x \geq 1 \\ ax, & |x| \leq 1 \\ bx - a + b, & x \leq -1. \end{cases}\quad (8b)$$

α , β , a , and b are parameters defined in terms of the original circuit parameters, and τ is a normalized time.

The system possesses three distinct saddle foci, one in the interior of each region (in particular, one at the origin, and the other two odd-symmetrically related and located at $(\pm k, 0, \mp k)$, where $k = (b - a)/(b + 1)$). Because of the piecewise-linear nature of the vector fields, a precise analysis of the qualitative dynamics in each region is tenable. This, coupled with the parameterization of the vector fields, makes it possible to establish formally the existence of an odd-symmetrically related pair of homoclinic orbits \mathcal{H}^\pm based at the origin. This nontrivial demonstration was first done in [8].

Fig. 7 is a computer-generated illustration of one such homoclinic orbit, with the following parameter values in (8):

$$\begin{aligned}\alpha &= 11.5996022, & \beta &= 15, & a &= m_0 = -1.142857143, \\ b &= m_1 = -0.7142857143\end{aligned}\quad (9)$$

and with an initial condition of

$$\begin{aligned}x(0) &= 0.00866911, & y(0) &= 0.000958759, \\ z(0) &= -0.00489156.\end{aligned}\quad (10)$$

The integration was performed on an IBM-compatible personal computer using the INSITE software package,³ employing a Runge-Kutta-Fehlberg-45 routine with an absolute and relative tolerance of 10^{-7} and 10^{-8} , respectively. Although we encourage readers to replicate this simulation, we caution them that this is a delicate and sensitive operation. In general, the reason for this sensitivity is that the spiral portion of the homoclinic orbit quickly escapes the *stable manifold* $W^c(\mathbf{0})$ [this manifold is the nonlinear *generalization* of the eigenplane $E^c(\mathbf{0})$], since it is a 2-D subset of the 3-D space and any computer has only finite precision.⁴ As a result, one can follow

³This software is a user-friendly analysis tool for nonlinear systems designed for the nonspecialist (see [9]).

⁴For the piecewise-linear system considered here, $W^c(\mathbf{0}) = E^c(\mathbf{0})$ in the interior of the inner region (where $|x| \leq 1$) that contains $\mathbf{0}$.

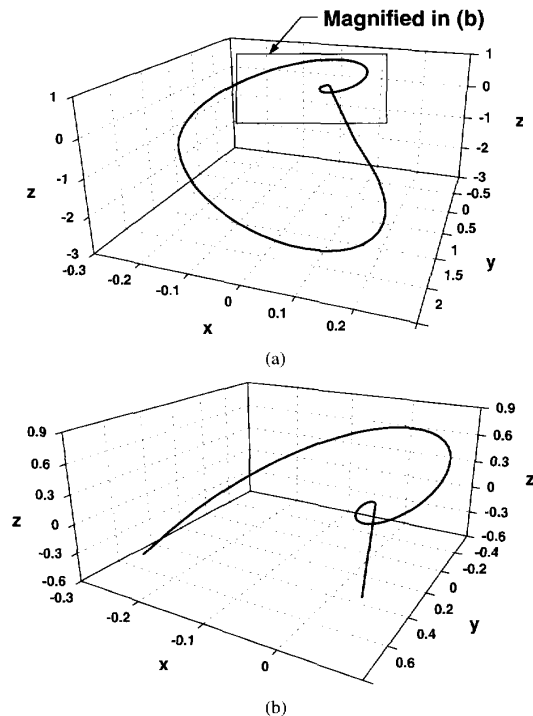


Fig. 7. Numerical simulation of a homoclinic orbit in the dynamics of Chua's circuit (see Example 2.1). (a) A view of the complete orbit. (b) A magnified view of the orbit near the equilibrium point at the origin.

such an orbit for only a moderate amount of time before the simulation begins to veer away into another set of dynamics. This latter effect can be seen in Fig. 8(a). Fig. 8(b) and (c) show what occurs when a parameter such as α is slightly perturbed from its nominal value given in (9). Observe how the orbit is deflected either above or below $W^c(\mathbf{0})$ and thus does not form a closed orbit. Conversely, by the continuity of solutions of differential equations with respect to their parameters, one could use these opposing-orbit deviations to argue intuitively for the existence of some homoclinic orbit in the dynamics of (8).

The numerical sensitivity issues and intuitive arguments just discussed indicate that a rigorous proof is needed to ensure the existence of such an orbit, as was performed in [8]. With the parameters in (9), one also finds that the characteristic eigenvalues of the origin are

$$\gamma = 2.9399 \text{ and } \sigma \pm j\omega = -1.1414 \pm j2.6743 \quad (11)$$

thus satisfying the Shil'nikov inequality in (5). An application of the extended homoclinic Shil'nikov method (see Remark i) to Theorem 2.1 to this system then proves the existence of chaos in (8).

Theorem 2.2 (Heteroclinic Shil'nikov Method): Given the third-order autonomous system in (1), where ξ is as in Theorem 2.1. Let \mathbf{x}_{e1} and \mathbf{x}_{e2} be two distinct equilibrium points for (1). Suppose the following:

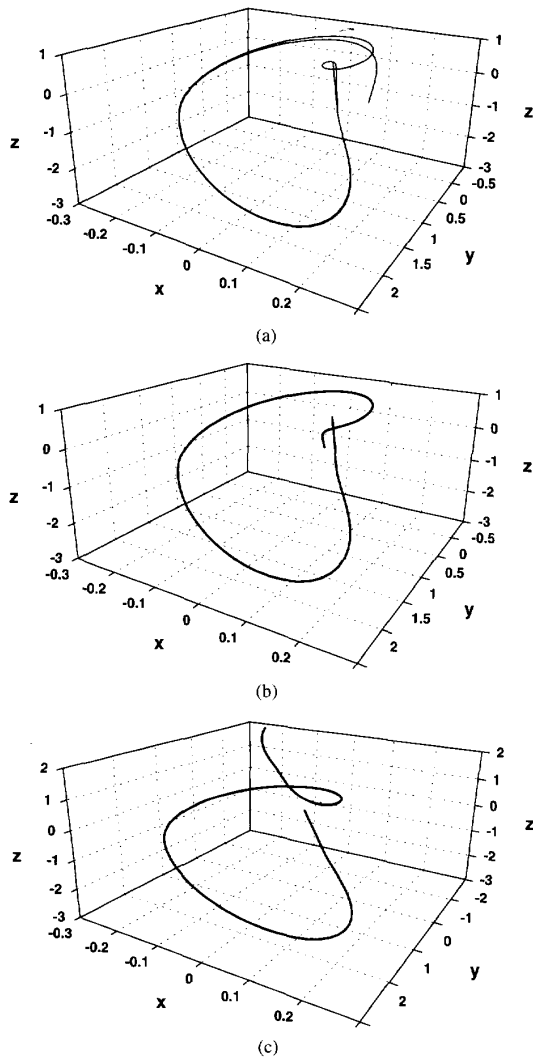


Fig. 8. Illustration of the sensitivity of the homoclinic orbit observed in Fig. 7 to finite numerical precision and small parameter perturbations. (a) Simulation resulting from letting the integration continue for a longer period of time than in Fig. 7(a). Ideally, the spiral portion of the orbit should take an infinite amount of time to reach the equilibrium point. Instead, finite computer error causes this orbit to deviate from its properly closed form. (b) Simulation resulting from perturbing the parameter α to the slightly lower value of 11.598. Observe how the orbit is deflected below the 2-D stable manifold $W^c(0)$. (c) Simulation resulting from α being increased to the value of 11.61. In this case, the trajectory is deflected above $W^c(0)$.

- 1) Both \mathbf{x}_{e1} and \mathbf{x}_{e2} are saddle foci that satisfy the Shil'nikov inequality

$$|\gamma_i| > |\sigma_i| > 0 \quad (i = 1, 2) \quad (12a)$$

with the further constraint

$$\sigma_1\sigma_2 > 0 \text{ or } \gamma_1\gamma_2 > 0. \quad (12b)$$

- 2) There is a heteroclinic loop \mathcal{H}_l joining \mathbf{x}_{e1} to \mathbf{x}_{e2} that is made up of two heteroclinic orbits $\mathcal{H}_i (i = 1, 2)$.

Then, conclusions 1–3 of Theorem 2.1 hold again, with \mathcal{H} replaced by \mathcal{H}_l , the equilibrium point \mathbf{x}_e by $\mathbf{x}_{ei} (i = 1, 2)$, and homoclinic chaos by the corresponding term *heteroclinic chaos*.

Remarks

i) This result is a generalization of the basic finding of Shil'nikov. Like Theorem 2.1, it has also been extended to the piecewise- C^2 case with the requirement that 1) each equilibrium point be in the interior of a piece (this could be the same piece for both points), and 2) the heteroclinic orbits be bounded away from any equilibria other than \mathbf{x}_{ei} and not be tangent to any boundary surface of any piece. Again the details can be found in [6].

ii) Remarks similar to ii) through iv) above hold here as well.

Example 2.2 (Chua's Circuit: Heteroclinic Orbit Between Two Saddle Foci): The double-hook vector-field family is closely related to its double-scroll counterpart. In fact, the major difference between the vector field families is that the origin for (1) is a *saddle-node* equilibrium point instead; that is, the characteristic eigenvalues of $D\xi(\mathbf{x}_e)$ are all real, nonzero, and not all of the same sign. The experimental, simulative, and analytical aspects of the double-hook dynamics can be found in [10] and [11] and in the detailed dissertation of [12]. In this case, a single odd-symmetric heteroclinic loop \mathcal{H}_l that joins the outer two saddle foci (similar to the loop illustrated in Fig. 2(b)) is analytically found to be a first-order fixed point of an appropriate Poincaré map constructed to characterize the double-hook system. Then the extended heteroclinic Shil'nikov method (see Remark i) to Theorem 2.2) is applied to a parameterized version of the system to conclude formally that chaos is present.

The computer simulations in Fig. 9, which are analogous to Figs. 7 and 8 for the homoclinic orbit in Chua's circuit, illustrate 1) the heteroclinic loop \mathcal{H}_l , which consists of two homoclinic orbits and 2) the sensitivity of the simulations to small perturbations in the parameter α . These simulations turn out to be even more difficult to perform than those for the homoclinic-orbit case, since \mathcal{H}_l connects the two widely separated (with respect to finite-precision concerns) saddle foci⁵

$$\mathbf{x}_{ei} = (\pm 22.32, 0, \mp 22.32)^T, \quad i = 1, 2 \quad (13)$$

which are separated by a Euclidean distance of 63.13... In addition, $\mathbf{x}_{ei} (i = 1, 2)$ has reversed stability (that is, σ and γ have changed sign) compared to the saddle focus at the origin in Example 2.1 above (consider (11), and (16), below). Consequently, we also had to perform our simulations in reverse time, that is, with the right-hand side of (8a) reversed in sign.

The presentation of \mathcal{H}_l in Fig. 9(a) was developed with the following parameter values:

$$\begin{aligned} \alpha &= -4.50746268737, & \beta &= -3.3373353844, \\ a &= -2.4924, & b &= -0.93 \end{aligned} \quad (14)$$

⁵Note that the upper (lower) signs in (13) correspond to $i = 1, 2$. This convention holds throughout.

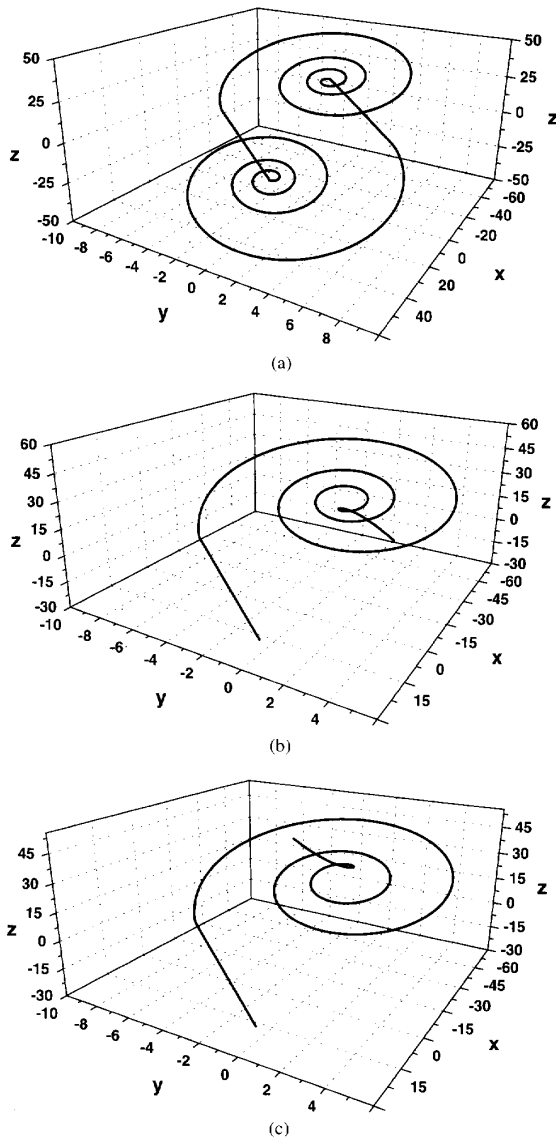


Fig. 9. Simulations associated with heteroclinic orbits in Chua's circuit (see Example 2.2). (a) The complete heteroclinic loop connecting the two saddle foci in (13). (b) For the slightly higher α value of -4.50746269 , note how the orbit is deflected below the 2-D manifold $W^c(\mathbf{x}_{e2})$. (c) The deflection above $W^c(\mathbf{x}_{e2})$ caused by the slightly lower α value of -4.50746260 .

and with the following two initial conditions (one for each orbit):

$$\mathbf{x}_i(0) = (\pm 22.2861576, \mp 0.009506608, \mp 22.28662665)^T, \quad i = 1, 2. \quad (15)$$

In this case, the absolute and relative error tolerances were taken to be 10^{-10} and 10^{-11} , respectively. Even with these tight bounds, a finite final time of 26.2 had to be employed in order for the orbits not to escape from the stable (with respect

to reverse time) manifold⁶ $W^c(\mathbf{x}_{ei})$ because of numerical error. Fig. 9(b) and (c) illustrate the deflection of the orbit initiating at the point $\mathbf{x}_1(0)$ in (15) above and below $W^c(\mathbf{x}_{e2})$ (with respect to the z -coordinate) when α is slightly changed from its value in (14). This reflects the extreme sensitivity of these simulations to parameter perturbations. In this case the characteristic eigenvalues for \mathbf{x}_{ei} ($i = 1, 2$) are given by the single set

$$\begin{aligned} \gamma_i &= -0.9506607987, \\ \sigma_i \pm j\omega_i &= 0.1330915934 \pm j1.044002616, \\ & i = 1, 2 \end{aligned} \quad (16)$$

and are seen to satisfy the necessary conditions in (12) of Theorem 2.2.

III. CONCLUSION

This paper has given a brief introduction into the method of Shil'nikov used to detect analytically the presence of chaos in continuous autonomous systems. This powerful tool should be employed whenever possible, since the nature of chaos can make it precarious to rely simply on experimental measurements or computer simulations—which are subject to limitations on time duration, bandwidth, and numerical precision. This tutorial should serve as a springboard to study this diagnostic further, so that its importance and potential can be appreciated, as well as to obtain the detailed information needed for its hands-on application (the books by Wiggins [1], [4] are highly recommended). In fact, it has been conjectured that lurking behind most chaotic behavior is the existence of some homoclinic orbit or heteroclinic loop, making the significance of the Shil'nikov approach quite evident. If such pursuits are undertaken, be forewarned that the field of nonlinear dynamics is engaging and exciting, and that the nonlinear toolkit has many more tools with which one can gain insight into the challenging problems currently arising in a whole spectrum of fields.

ACKNOWLEDGMENT

The author thanks those people at The Aerospace Corporation who supported him in the writing of this special journal issue paper, especially M. T. Meyer for his editorial assistance, Dr. J. D. Michaelson for his support, and A. M. Young for his useful suggestions to improve the readability of this paper for the nonspecialist. He also thanks C.-W. Wu of the Electronics Research Laboratory, University of California at Berkeley, for providing assistance on some of the numerical simulations included in this paper.

REFERENCES

- [1] S. Wiggins, *Introduction to Applied Nonlinear Dynamical Systems and Chaos*, Vol. 2, *Texts in Applied Mathematics*. New York: Springer-Verlag, 1990.
- [2] L. P. Shil'nikov, "A case of the existence of a countable number of periodic motions," *Sov. Math. Doklady*, vol. 6, pp. 163–166, Jan.–Feb. 1965 (translated by S. Puckette).

⁶Like $W^c(0)$ in Example 2.1, $W^c(\mathbf{x}_{ei}) = E^c(\mathbf{x}_{ei})$ here for the outer regions (where $|x| \geq 1$) that contain \mathbf{x}_{ei} .

- [3] L. P. Shil'nikov, "A contribution to the problem of the structure of an extended neighborhood of rough equilibrium state of saddle-focus type," *Math. U.S.S.R.—Shornik*, vol. 10, pp. 91–102, Jan.–Feb. 1970 (translated by F. A. Cezus).
- [4] S. Wiggins, *Global Bifurcations and Chaos, Applied Mathematical Sciences*. New York: Springer-Verlag, 1988, vol. 73.
- [5] S. Smale, "Diffeomorphisms with many periodic points," in *Differential and Combinatorial Topology* (S. S. Cairns, Ed.). Princeton, NJ: Princeton Univ. Press, 1965, pp. 63–80.
- [6] C. Tresser, "On some theorems of L. P. Shil'nikov and some applications," preprint, Univ. of Nice, France, 1982; also abridged form in *Annales l'Inst. Henri Poincaré*, vol. 40, pp. 441–461, 1984.
- [7] L. O. Chua, "The genesis of Chua's circuit," *Int. J. Electron. Commun.*, vol. 46, no. 4, pp. 250–257, 1992.
- [8] L. O. Chua, M. Komuro, and T. Matsumoto, "The double scroll family," *IEEE Trans. Circuits Syst.*, vol. CAS-33, pp. 1072–1118, Nov. 1986.
- [9] T. S. Parker and L. O. Chua, *Practical Numerical Algorithms for Chaotic Systems*. New York: Springer-Verlag, 1989.
- [10] P. Bartissol and L. O. Chua, "The double hook," *IEEE Trans. Circuits Syst.*, vol. 35, pp. 1512–1522, Dec. 1988.
- [11] C. P. Silva, "The double-hook attractor in Chua's circuit: Some analytical results," in *Chua's Circuit: A Paradigm for Chaos* (R. N. Madan, Ed.). Singapore: World Scientific, 1993.
- [12] C. P. Silva, "Chaos in the double-hook family: An application of Shil'nikov theory," Ph.D. dissertation, Univ. of California, Berkeley, May 1993.



Christopher P. Silva (S'81–M'89) was born on March 17, 1960 in Fortuna, CA. He received the B.S., M.S., and Ph.D. degrees, all in electrical engineering, in 1982, 1985, and 1993, respectively, from the University of California, Berkeley. His graduate work was supported mainly by a National Science Foundation Fellowship and a Lockheed Leadership Fellowship.

He is a Member of the Technical Staff of the Communications Electronics Department, Communications Systems Subdivision, at The Aerospace Corporation, Los Angeles. He has been the principal investigator on several internally funded research projects addressing nonlinear microwave CAD, secure communications by means of chaos, and compensation of nonlinear satellite communications channels. In addition, he is involved with the modeling of nonlinear wave propagation in a cryogenic acoustic microscope, the investigation of ion beam distribution issues in cesium atomic frequency standards, and the application of wavelet analysis to CAD. Previously, he worked as a Post-Graduate Researcher at the Electronics Research Laboratory, University of California, Berkeley, where he investigated the chaotic dynamics of nonlinear circuits and systems.

Dr. Silva is a member of Eta Kappa Nu, Tau Beta Pi, Phi Beta Kappa, the Society for Industrial and Applied Mathematics, and the American Mathematical Society.